

Spectral Roll-off Points: Estimating Useful Information Under the Basis of Low-frequency Data Representations

Yunkai Yu ^{*1} Zhihong Yang ^{*2} Yuyang You ¹ Guozheng Liu ¹ Peiyao Li ^{3,4} Zhicheng Yang ⁵ Wenjing Shan ¹

Abstract

Useful information is the basis for model decisions. Estimating useful information in feature maps promotes the understanding of the mechanisms of neural networks. Low frequency is a prerequisite for useful information in data representations, because downscaling operations reduce the communication bandwidth. This study proposes the use of spectral roll-off points (SROPs) to integrate the low-frequency condition when estimating useful information. The computation of an SROP is extended from a 1-D signal to a 2-D image by the required rotation invariance in image classification tasks. SROP statistics across feature maps are implemented for layer-wise useful information estimation. Sanity checks demonstrate that the variation of layer-wise SROP distributions among model input can be used to recognize useful components that support model decisions. Moreover, the variations of SROPs and accuracy, the ground truth of useful information of models, are synchronous when adopting sufficient training in various model structures. Therefore, SROP is an accurate and convenient estimation of useful information. It promotes the explainability of artificial intelligence with respect to frequency-domain knowledge.

1. Introduction

Useful information, also named as *actionable information* (Xu et al., 2020b), is an empirical concept. In this paper, information that supports model decision is defined as useful information (Sec. 3). From a results-oriented view, performance indicates the ground truth of useful information

^{*}First co-authors ¹Beijing Institute of Technology, Beijing, China ²Institute of Medicinal Plant Development, Chinese Academy of Medical Sciences, Beijing, China ³Tsinghua University, Beijing, China ⁴Global Health Drug Discovery Institute, Beijing, China ⁵PAII Inc, Palo Alto, USA. Correspondence to: Yuyang You <arthurwy@163.com>.

The template is a modification of the ICML 2020 template.

in models. Deep neural networks (DNNs) are effective at extracting useful information given their remarkable success in a broad range of real-world tasks. However, a lack of generalization measures (Jiang et al., 2020) makes the estimation of useful information in DNNs difficult. Modeling the important property of useful information can exclude redundant information. The sampling theorem states that downscaling blocks in DNNs, which always halve the spatial resolution (sampling frequency), will reject the high-frequency information in feature maps (Cover & Thomas, 1990; Shannon & Weaver, 1949). Therefore, useful information can survive from downscale steps when it is of low frequency in data representations. This property is denoted as low-frequency prior (LFP). Notably, the "high frequencies" in LFP are defined by spatial resolutions rather than in common usage (textures): e.g. there is no high frequencies (25-50 Hz) in a $\mathcal{R}^{1 \times 50}$ feature map when the input is a \mathcal{R}^{100} signal. On the basis of LFP, we propose the use of spectral roll-off points (SROPs), which quantify feature energy in low-frequency bands, to estimate useful information. The use of SROPs is an easy-to-follow scheme to estimate useful information of DNNs by leveraging enriched frequency-domain knowledge.

Some obstacles in computation need to be tackled to estimate layer-wise useful information. Because obtaining a SROP requires a 1-D spectrum of a 1-D signal. Transforming the 2-D spectrum to 1-D spectrum via a radial average method enables us to extend the SROP computation to a 2-D feature map. This modification is consistent with the desired property in image classification tasks that DNNs possess rotation invariance (Dieleman et al., 2016; Goodfellow et al.; Lenc & Vedaldi, 2015). Considered that there are usually tens of 2-D feature maps in a DNN layer, SROP statistics like mean values are adopted in the estimation of useful information. This design substantially simplifies the computation and proves to be feasible in experiments.

Experiments are designed to provide empirical evidence that SROPs can distinguish the variations of useful information. Three factors that relate to useful information, model input, model structures and sufficient training, are summarized from previous work (Goodfellow et al.; Koh & Liang, 2017; Larochelle et al., 2007; Yak et al., 2019). Control

experiments are designed under the sanity check framework (Adebayo et al.). Everyday-object and digit images are synthesized with different proportions, which lead to variations from different useful image patterns and noise intensity. The SROPs of model representations change synchronously. The use of SROP statistics explains the effectiveness of downscaling, batch normalization (BN), anti-aliased blocks and intermediate layers. Layer-wise SROP curves visualize the flows of useful information in multiple modern model architectures. Preserving much information at early stage is a common strategy for DNNs to achieve satisfying performance. Comparisons between randomized and pre-trained models demonstrate that low-frequency data representations are the results of sufficient training. A finding is that the loss of high-frequency components from downscaling operations is negligible for data representations in trained models. Variations of SROPs and useful information are proved to be consistent. The use of SROPs improves the explainability of DNNs. The application scope of SROPs is discussed in Sec. 7.

Our contributions are summarized as follows:

- We propose the use of SROPs in the evaluation of useful information by modeling LFP. The computation of SROPs is extended from a 1-D signal to DNN feature maps. Consequently, we can explain layer-wise useful information with frequency-domain knowledge.
- Systematic analysis of layer-wise useful information proves that SROP can distinguish the variations of useful information derived from different model input, model structures and sufficient training. Experiments include 20 modern DNNs and 3 large-scale datasets.
- SROP separates redundant information from useful information. Theoretical analysis and empirical evidence reveal the potential of SROPs in adversarial learning, model optimization, and dataset evaluation.

2. Related work

Useful information and redundancy coexist in DNN representations and are assessed together in current metrics that evaluate information. We demonstrate the essence of modeling useful information by LFP, and refer to current research on frequency analysis.

2.1. Metrics of evaluating information

Many approaches evaluate transmissible information. Shannon mutual information measures the entropy variation between two variables. Therefore, entropy including Renyi and H entropy (DeGroot, 1962; Lenzi et al., 2000), associates the information to prediction loss. However, using these metrics in high dimension meets difficulties in

computation. \mathcal{V} -predictive information (Xu et al., 2020b) concentrates on actionable information. It calibrates mutual information through an additional benchmark entropy from natural random process and extends the application scope. Mutual information measures the useful information in model input (Cheng et al., 2020; Liang et al., 2020). However, the outputs of different DNN layers contain spurious causal relationships. It indicates that computing mutual information with variables in different layers may capture spurious causal relationships. Additional prior knowledge is needed for mutual information (Negrea et al.).

Assessing the representational capacity of a hidden layer is another method to evaluate existing information in DNN feature maps. Intrinsic dimensionality (ID) is the minimal number of base vectors to reconstruct hidden manifold. Projection methods search a best subspace based on the projection error or local connectivity to compute ID (Abdi & Williams, 2010; Tribello et al., 2012). Nearest-neighbour ID estimators infer the fractal dimension by first neighbors under the assumptions of data neighbourhood distribution (Badii & Politi, 1984). A recent TWO-NN estimator shows a satisfactory universality (Facco et al., 2017). As a statistical method, the accuracy of ID estimation is inevitably compromised by the scale and heterogeneity of datasets.

Ignoring LFP is the foremost problem of mutual information and ID when estimating useful information. The consequence is that noise and redundancy, which are common in DNNs (Frankle & Carbin, 2019), are counted as useful components. On the basis of LFP, useful information is recognized as low-frequency representations, which inspires the use of SROPs.

2.2. Importance of LFP

LFP guarantees the decrease in spatial resolution of feature maps. Prior knowledge in frequency domain has a more intuitive relation with spatial resolution compared to low-dimension prior that probability mass concentrates near regions with a much smaller dimensionality than the original space where the data live (Bengio et al., 2013). The redundancy in high-frequency band motivates a sparse sampling method in feature maps to reduce computation (Xie et al., 2020). Moreover, useful low-frequency data representations are desired to ensure that useful information passes through downscaling layers according to LFP. Anti-aliased models implement additional low-pass filters in downscaling blocks but received unexpected improved model performance (Zhang, 2019). Kernel smoothness is highlighted in encoding high-frequency patterns in images and adversarial learning (Xu et al., 2020b). These works capture sufficient useful information and address the importance of LFP. Hence, prioritizing the important property (LFP) by the use of SROPs in the estimation of useful in-

formation is feasible and promising. Frequency domain knowledge provides DNNs with good interpretability.

2.3. Frequency analysis of data representations

Frequency analysis points out the importance of low-frequency components in model input. It's found that DNNs firstly learn low-frequency components of model input during training process (Xu et al., 2019; 2018). The *spectral bias* indicates that high-frequency functions of input can be expressed by low frequency network functions defined in hidden manifolds (Rahaman et al., 2019). Optimisation procedure is content-aware, where learning simple patterns of the data is the priority (Arpit et al., 2017). Low-frequency patterns are simple. Consequently, a data representation of low frequency is produced after training. Our study leverages the good interpretability of frequency-domain knowledge to derive an applicable measure of useful information in DNN feature maps.

3. Preliminaries

Ground truth of useful information: The ground truth of useful information is given by its desired properties. According to human ingenuity, model performance can be used as the ground truth of useful information in DNN, because satisfying model performance indicates sufficient useful information in model. Useful information is content-aware. Therefore, modifying model input is a strategy to provide a useful information variation in DNN feature maps. Details can be found in Sec. 5.1. Another property is that useful information along depth is non-increasing. It can be used to discover the redundancy in estimation Sec. 6.3.

Notations of DNN: Throughout the paper a neural network backbone F is denoted as a consequence of L hidden layers $\{T_1, T_2, \dots, T_L\}$ as follows:

$$F(X) = (T_L \circ T_{L-1} \circ \dots \circ T_1)(X), \quad (1)$$

where X is the model input. The output of the k^{th} layer Y_k is defined as $Y_k = (T_k \circ T_{k-1} \circ \dots \circ T_1)(X)$. Y_k is a $c_k \times n_k \times n_k$ vector, composed of c_k 2-D feature maps.

Notations of layers: The notations of layers are shown in Table 1. The kernel sizes of the pooling layers are two except for those of AlexNet and DenseNet, where the kernel size is three. The convolutional blocks in AlexNet and VGG16 contain a convolution and an activation function ReLU, while other convolutional layers have an additional BN layer. The pooling layers and stride-convolutions in anti-aliased models behave differently (see Sec. 3).

Anti-aliased blocks: Anti-aliased blocks in this study improve downscaling operations to make DNNs shift-invariant.

They use a dense max-pooling layer to obtain an intermediate signal. Afterwards, the intermediate signal is down-scaled by a blur-pooling layer to gain the final output. The blur pooling layer in this paper is equivalent to the bi-linear downsampling method. The effectiveness of the design is validated in large-scale databases like CIFAR10 and ImageNet (Krizhevsky, 2012; Russakovsky et al., 2015). More details may be found in (Zhang, 2019).

4. Methods

SROPs characterize 1-D signals. The computation of SROPs is extrapolated to multiple 2-D feature maps generated from DNN kernels to estimate layer-wise useful information. Radially averaged power spectrum enables us to calculate a SROP in a 2-D feature map. DNN kernels outputs 3-D feature maps. SROP statistics give insights in SROP distribution across kernels in the same layer. They are selected as the evaluation metrics of useful information.

4.1. SROPs of 1-D signal

SROPs are known to be high for right-skewed distributions (Scheirer & Slaney, 1997) and low when data representations contain increased low-frequency components. Useful information is available only in low-frequency representations when followed by a downsampling block, whereas redundant information distributes randomly. Theoretically speaking, low SROPs indicate that useful information is ideally compressed. The SROP of a 1-D signal is defined in Eq. 2.

$$\text{SROP} = \sum_{k=b_1}^{b_2} S_{1D}(k) = \kappa \sum_{k=b_1}^{b_2} S_{1D}(k), \quad (2)$$

where $S_{1D}(k)$ denotes the value of spectrum S_{1D} in bin k , and b_1 and b_2 are the edges of the frequency band. $\kappa = 0.85$ is a cut-off point of total energy. In this study, S_{1D} is a one-sided power spectrum density, which is expressed as

$$S_{1D}(k) = \frac{|\mathcal{F}(k)|}{\sum_{j=b_1}^{b_2} |\mathcal{F}(j)|}, \quad (3)$$

where $\mathcal{F}(k)$ is the k^{th} component of the Fourier sequence of input. To make fair SROP comparisons among samples with different spatial resolutions, we normalized SROPs to $[0, 1]$ as shown in Eq 4:

$$\text{SROP}_{\text{normalized}} = (\text{SROP} - b_1) / (b_2 - b_1). \quad (4)$$

4.2. Radially averaged power spectrum

We map the 2-D power spectrum to its radially averaged form to calculate the SROP of a 2-D image, which is based on the prior that well-trained models are useful for tasks require good rotational invariance. Actually, radially averaged SROP has been applied to estimate systematic errors

Backbone	AlexNet	VGG	ResNet		DenseNet
Output size		VGG16, VGG16-bn	ResNet18	ResNet34	
224 × 224	-	-	-	-	-
	-	conv0.0-conv0.1	-	-	-
112 × 112	-	pool1	-	-	-
	-	conv1.0-conv1.1	conv0	conv0	conv0
56 × 56	-	pool2	pool1	pool1	pool1
(55 × 55)	conv0	conv2.0-2.2	resblk1.0-1.1	resblk1.0-1.2	denseblk1
28 × 28	pool1	pool3	resblk2.0	resblk2.0	transblk1
(27 × 27)	conv1.0	conv3.0-3.2	resblk2.1	resblk2.1-2.3	denseblk2
14 × 14	pool2	pool4	resblk3.0	resblk3.0	transblk2
(13 × 13)	conv2.0-2.2	conv4.0-4.2	resblk3.1	resblk3.1-3.5	denseblk3
7 × 7	pool3	pool5	resblk4.0	resblk4.0	transblk3
	-	-	resblk4.1	resblk4.1-4.2	denseblk4, bn1

Table 1. Notations of backbones. Notably, the *convx,y* block in VGG16-bn has an additional BN layer compared to VGG16. The downscaled layers of original and anti-aliased models share the same notations and are highlighted in bold. The *denseblk* and *transblk* in DenseNet of different scales (DenseNet121, 169), also share the same notations.

in the noise levels of satellite images (Maus, 2008). A 2-D spectrum is denoted as $S_{2D} \in R^{n \times n}$ as $S_{2D}(r, \theta)$ in the polar basis, and the ordinate origin is at the center of the spectrum. After discretization, we obtain

$$m = \text{Floor}\left(\frac{\sqrt{2}(n-1)}{2}\right) - 1, \quad (5)$$

where m is the number of radius bins of discretized 1-D spectrum, and $\text{Floor}(\cdot)$ takes the nearest integer value of input towards minus infinity. Subsequently, we establish a mapping relation to transform a 2-D spectrum S_{2D} to 1-D spectrum $S_{1D} \in R^{1 \times m}$, which can be formulated as

$$S_{1D}(k) = \sum_{\theta=0}^{2\pi} S_{2D}(r_k, \theta), k \leq r_k < k+1, k \in [0, m], \quad (6)$$

where $m \approx n \times 0.7$ when n is large, suggesting a significant dip in the upper bound of frequency. This finding shows that the rotation invariance is a strong constraint. When $X \rightarrow \text{Rotate}(X)$, we have

$$S_{2D}(r, \theta) \rightarrow S_{2D}(r, \theta + \Delta\theta), S_{1D}(k) \rightarrow S_{1D}(k), \forall k. \quad (7)$$

Therefore, rotating a 2-D image will rotate the 2-D spectrum S_{2D} , but the radially averaged 1-D spectrum S_{1D} stays identical because it is independent with θ .

4.3. SROP statistics

DNN layers usually contain at least tens of filters. SROP distribution across kernels gives a comprehensive vision of layer-wise useful information. SROP statistics present the layer-wise useful information concisely. Kernel outputs of satisfactory model are concentrated. Accordingly, a small internal covariate shift is encouraged (Ioffe & Szegedy, 2015).

It indicates that SROPs among kernels are close to their mean values for trained models. For the reason, SROP *mean* value is used as the estimation of layer-wise useful information for the output Y_k . Median values are used, because their small deviations of mean values ensure that SROPs are concentrated. The use of SROP statistics has risk of loss of information in the layer-wise SROP distribution and may fail to differentiate situations with different amounts of useful information. Thus, in Sec. 7, we analyze the feasibility of using SROP statistics with results from sufficient experiments.

5. Experiment designs

SROPs in data representations are designed to reflect the variations of useful information. The data and model randomized tests (Adebayo et al.) are implemented to assess the correctness of SROPs.

5.1. Useful information variations from model input

Different noise intensity and diverse patterns in model input lead to variations in useful information of model representations. This experiment is to demonstrate that SROPs can distinguish useful patterns in feature maps that support model decision. Our method is to synthesize a frog image to MNIST digit images, and observe the SROPs in model representations among samples as illustrated in Fig. 1. To determine if the frog image can produce useful data representations, we design two cases when exploring the SROP variations from different model input. The cases are as follows:

- CASE I: The frog image is embedded into samples of category "1", $P(\text{label} = 1 | \text{frog} + \text{digit}) = 1$;

- CASE II: The frog image is embedded into all digit images, $P(\text{label} = 1 | \text{frog} + \text{digit}) = \text{unknown}$.

The frog image enables models to make correct decisions in CASE I, because it provides useful patterns as easy-to-learn hints to recognize samples in category "1". However, models are less likely to learn patterns of category "1" when an image "1" is of smaller proportion (higher w). Meanwhile, the frog image is noise in CASE II, which erodes useful digit patterns. In this way, the proportion of digit images $1 - w$ can be used as the ground truth of useful information in model input and feature maps. We train a CNN (inp) for 20 epochs with a learning rate of 0.001, and observe SROP statistics of its last convolution. The frog image has the highest SROP among CIFAR10 samples. Outputs of the convolution when using the frog image as input are called frog patterns and its SROP statistics is used as baselines. The SROPs of frog patterns in CASE I and II depend on usefulness of the same input if they are good estimation of useful information.

5.2. Useful information variations from model structures and sufficient training

Downscaling layers lead to a sharp spatial resolution decline, and intermediate layers would modify data representations. Layer-wise SROP statistics from various model structures are analyzed. A max-pooling block, where the stride and kernel size are both two, is used as the benchmark downscaling structure. Baseline SROPs are calculated by replacing intermediate layers with the benchmark structure. This process explores how intermediate layers facilitate the learning process by modifying data representations. The experiments include model structures like convolutions, max-pooling layers, blocks from ResNet and DenseNet, and anti-aliased blocks. Different model structures differentiate the useful information in data representations. The SROPs are supposed to behave differently.

Pre-trained models preserve more useful information than untrained models because they are sufficient trained. Therefore, we compare randomized and pre-trained models to analyze the effectiveness of sufficient training. The lack of useful information in training dynamic prevents us from validating SROP in training progress. Models pre-trained on ImageNet are from PyTorch (Paszke et al.) and Zhang (Zhang, 2019). SROP curves visualize the SROP variation along depth, which makes it possible to explore the effect of model architectures. A known observation is that an increasing depth or width in a model would ease the extraction of useful information (Rahaman et al., 2019). Moreover, the accuracy gain from increased model complexity will diminish for large models (Goodfellow et al.; Tan & Le, 2019). We expect SROP analysis to make these observations about useful information explainable.

6. Results

6.1. SROP variations from model input

SROP variations from different useful patterns: Digit and frog patterns are different useful patterns in CASE I. SROP distribution among samples is capable of reflecting the variation in model input. Fig. 1 demonstrates that the kernel density (KDE) plot of SROPs of model representations among the overall frog+digit samples w . Especially, in CASE II, the SROPs of model representations rise to 1 when noise destroys useful patterns completely ($w = 1$), as shown in the rightmost column. Digit patterns ($w = 0$) has three peaks. Two low-SROP peaks is a characteristic when using useful frog patterns ($w = 1$, CASE I). The SROP distributions in transition states ($0 < w < 1$, CASE I) may have either two or three low-SROP peaks. However, KDE plots with noisy input are likely to have additional peaks at high SROPs, as shown in CASE II. SROP distribution among samples can distinguish the variation from useful patterns in model input. The phenomena support the idea that SROP can be used to estimate useful information in feature maps.

SROP variations from different noise intensity: Fig. 2 demonstrates that SROPs in feature maps are sensitive to noise intensity. The mean SROP of the frog representations increases monotonically when w is larger than 0.5 in CASE II. Meanwhile, a significant accuracy drop occurs when w increases from 0.8 to 0.9. As a comparison, the same image generates low-SROP representations when it provides useful information in CASE I. SROPs have a negative correlation with noise intensity in model input.

6.2. SROP variations from model structures and sufficient training

Fig. 3 demonstrates the SROP variations caused by downscaling blocks and a BN layer. Fig. 4 visualized untrained and pre-trained SROP profiles of various models and the simulation results of replacing intermediate layers by benchmark pooling. We can report the SROPs in the useful information variation caused by model architectures and sufficient training.

With and without downscaling blocks/a BN layer: SROPs from max-pooling layers with large kernel size (3) edge close to the baseline (*kernel size* = 2) at a small output size in AlexNet. This confirms that large kernel size produces low SROPs in randomized blocks.

The only difference between VGG16 and VGG16-bn blocks is a BN layer. Outputs of layers with a BN block have small SROP inter-quartile ranges in outputs, indicating that BN makes the layer-wise output more concentrated compared with the condition without BN. From the view of SROPs,

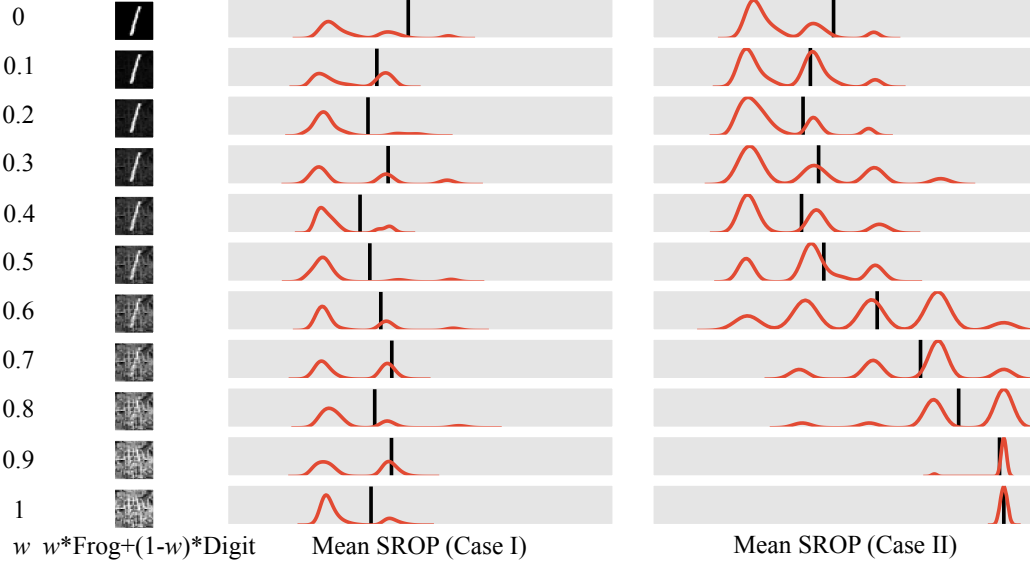


Figure 1. Frog/digit images and SROP distributions. w indicates the proportion of the frog image in synthesized images. The frog image is useful information in CASE I and noise in CASE II when performing the digit classification task. Red plots are the mean SROPs' kernel density plots of the convolution when using the MNIST test set as model input. The models are trained. Vertical lines are mean SROPs when using the frog image as model input. Details of CASES I and II and the convolution can be found in Sec. 5.1.

BN reduces the internal covariate shift (Ioffe & Szegedy, 2015).

With and without anti-aliased/intermediate layers: Different SROP profiles are observed when using anti-aliased and intermediate layers. It's known that anti-aliased layers output anti-aliased and useful feature maps. Compared with the origin models, variations of useful information and SROPs are both observed. A finding is that pre-trained anti-aliased layers can preserve more high-frequency components at initial layers rather than loss information despite employing additional low-pass filters. In particular, the mean SROP values of *resblk1.1* in randomized and pre-trained anti-aliased ResNet18 are almost the same. Low SROPs indicate satisfactory low-frequency data representations. Anti-aliased models have low SROPs at the end of the hidden layer except for AlexNet, which is in accordance with their excellent performance.

Intermediate layers improve lower-frequency representations when the spatial resolution stays constant. This is reflected in lower SROPs in the downscaling layers when intermediate layers are provided. For instance, SROPs in *resblk1.0* grow higher after applying *resblk1.1*, but pre-trained intermediate layers enable lower SROPs in *resblk2.0* compared with downscaling directly with the benchmark. This finding that intermediate layers affect the learnability of useful information can be reported in a SROP scheme. The increase of intermediate layers obtains smooth SROP profile, as shown by the SROP curves of ResNet18 and ResNet34.

SROP profiles and model architectures: The diversity of SROP profiles reflects the diversity of designs for improving the extraction of useful information. Untrained and pre-trained models possess similar SROP patterns. This condition indicates that model architectures predetermine the flow of useful information. The skip connection in the ResNet family injects high-frequency components, embodied as an uptrend in the layers of the same spatial resolution. Anti-aliased blocks induce different SROP patterns. Considering that the anti-aliased models surpass their original versions, we conclude that retaining sufficient high-frequency information at shallow layers is important.

Randomized and pre-trained models The SROP dip in deep layers is the main difference between the randomized and pre-trained models. The SROP discrepancy verifies that a well-trained model converts useful information to low-frequency representations.

Minimum mean SROPs and spatial resolution: Sufficient training increases the useful information in data representations, which is verified by decreasing SROPs. However, there exists a required low-end of spatial resolution to carry all useful information. Table 2 explores the minimum mean SROP at each output size across the architectures mentioned in Table 1. Modern pre-trained models can approximately cut SROP values in half compared with randomized models, especially when the output size is less than 56×56 . This condition indicates that low-frequency information will be

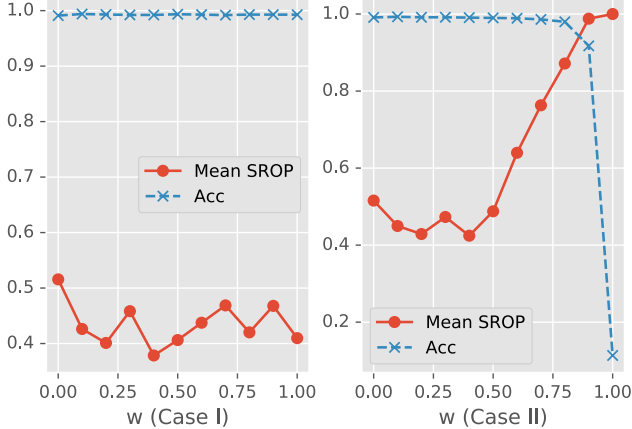


Figure 2. Accuracy and mean SROP in feature maps when using a frog image as input. The y-axis denotes their numerical values. As introduced in Sec. 5.1, the frog image provides useful information in CASE I and noise in CASE II, and mean SROP in feature maps stays low when model extracts sufficient useful information for high accuracy in CASE I. The model fails to yield ideal accuracy in CASE II, which is reflected in high SROPs.

perfectly preserved after successive downscaling blocks. The constraint of LFP encourages low-frequency representations before downscaling. It is true even for DenseNet and ResNet, where the downscaling layers can encode high-frequency components rather than maxpooling layers. Previous ideas emphasize the loss of high-frequency information caused by downscaling operations (Xu et al., 2020a; Zhang, 2019). However, our results show that the loss of useful information from downscaling steps is negligible due to intermediate layers. Given that all useful information is transmissible, additional filters are likely to introduce redundancy for large models. It may explain the diminishing accuracy gain from an increased model width. The minimum mean SROP is higher than 50% of the baseline when output sizes are larger than 56×56 , as shown in Table 2. This finding indicates that transforming high-frequency useful information to low-frequency representations is difficult at initial layers. Wang *et al.* encourage using smooth kernels to make models generalizable (Wang et al., 2020).

6.3. Comparisons between SROPs and ID

Layer-wise observation demonstrates the feasibility of SROPs when estimating useful information. Ansuini *et al.* reported hunch-backed layer-wise ID profiles. The largest ID is in the relative depth range of 0.2-0.4. Its value is approximately four times the ID at the first layer. Details about ID observations may be found in (Ansuini et al., 2019). Meanwhile, SROP profiles are concave, and the largest SROP value appears at initial layers. Considered that the information curve is supposed to be concave with a decaying spatial resolution (Shwartz-Ziv & Tishby, 2017),

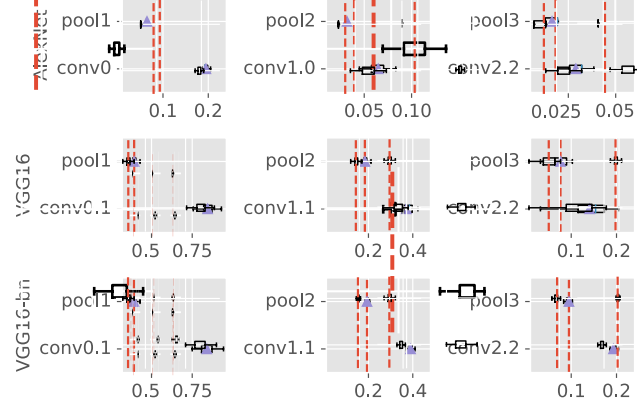


Figure 3. Normalized SROPs in pooling layers and randomized strided-convolutions. The kernel sizes of the pooling layers in AlexNet and VGG are three and two, respectively. Triangles denote the SROP mean values. Dashed lines denote the SROP mean values from the benchmark (Sec. 5.2).

SROPs contain less redundancy than ID when it is used as the estimation of useful information.

7. Discussion

Feasibility of SROP statistics: The feasibility of using SROP mean values is queried in Sec. 4.3 and validated in Sec. 6. Other SROP statistics can characterise layer-wise useful information from different perspectives. For instance, SROP variance and standard deviation measure the degree of kernel disequilibrium or the internal covariate shift in a DNN layer. In summary, SROP statistics are informative to describe useful information.

Potential applications of SROPs: Sec. 6.1 shows that different SROP distributions among samples indicate different useful input patterns in the overall dataset. Fig. 2 reveals the potential applications of SROPs in adversarial learning tasks, where recognizing useful information is important. Kernel smoothness in the first convolutions of DNN contributes to adversarial robustness (Wang et al., 2020).

Monitoring the training process is a potential use of SROP variance and standard deviation because a small internal covariate shift is a desired property for DNNs (Ioffe & Szegedy, 2015). Kernel-wise SROPs provide more detailed information compared with layer-wise SROPs. The useful information can be monitored channel-wisely, since SROP is a good estimation of useful information.

Another potential application of SROP distribution is to evaluate whether a customized dataset is feasible for deep learning tasks. Obtaining the same SROP distribution of mode representations as the benchmark database is a practical target for customized datasets. For instance, the peak

Output size	Baseline	Min mean SROP	Layer	Anti-aliased
224 × 224	0.852	0.494	conv0.1(VGG16-bn)	No
112 × 112	0.399	0.237	conv1.1 (VGG16-bn)	Yes
56 × 56 (55 × 55)	0.198	0.101	denseblk1 (DenseNet121)	Yes
28 × 28 (27 × 27)	0.098	0.047	conv1.0 (AlexNet)	Yes
14 × 14 (13 × 13)	0.048	0.023	conv4.2 (VGG16-bn)	No
7 × 7	0.025	0.012	resblk4.2 (ResNet34)	Yes

Table 2. The minimum mean SROP across model backbones pre-trained on ImageNet at different spatial resolutions. The output sizes of AlexNet feature maps are slight smaller, as displayed in brackets.

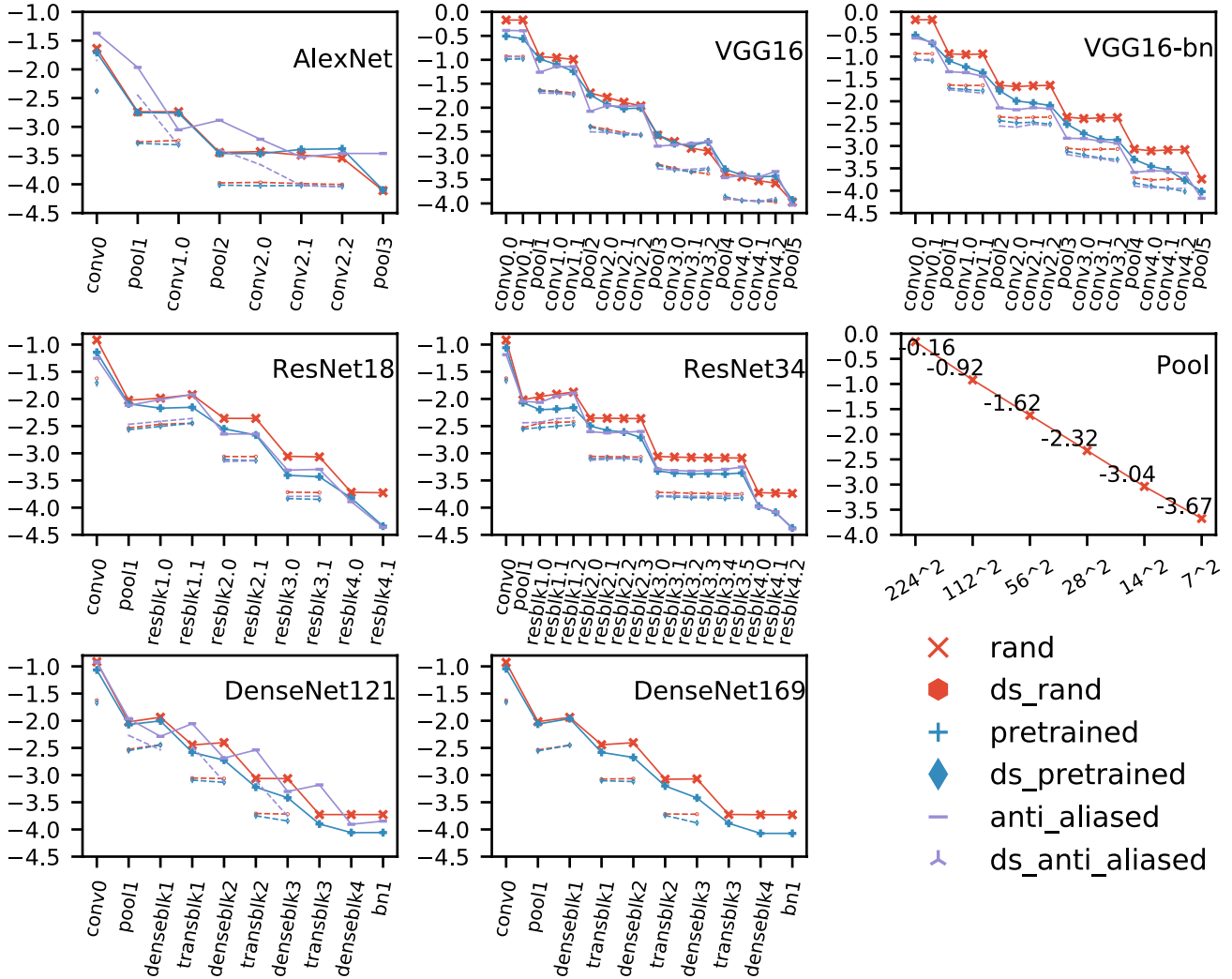


Figure 4. SROP mean values in randomized and pre-trained backbones. The y axis denotes $\log(SROP)$. Anti-aliased models are pre-trained. The benchmark *Pool* is a max-pooling layer whose kernel size and stride are two. SROP curves with the *ds* prefix are computed by replacing intermediate layers with the benchmark *Pool*.

with the highest SROPs in Fig. 1 when $w = 0$ is composed of 893 images of category "1" and tens of other digit samples when using the MNIST dataset. Therefore, images of category "1" should be collected if the high-SROP peak is not observed when using the customized digit dataset.

Limitations of SROPs and potential solutions: The use of SROPs is subject to some limitations. Distinguishing low-frequency disturbance and information is a question raised in Sec. 5.1. Expanding the spectral features of layer-wise SROP distributions is a possible solution to distinguish patterns of useful and irrelevant information. Another limitation is that SROP is only relevant for topologically ordered layers like convolutional layers, because LFP is only meaningful when neighbour pixels have spatial correlations. Extrapolating LFP to other model structures is a prerequisite when frequency domain knowledge is used to understand useful information.

8. Conclusion

A novel useful information estimation approach, the use of SROPs, is proposed on the basis of the important prior knowledge that data representations in DNNs are low-frequency dominated. To extend the implementation of SROPs from a 1-D signal to multiple 2-D feature maps, we utilize the prior knowledge that effective models should possess rotation invariance and small internal covariate shift. Sanity checks prove that SROP can accurately assess useful information. Because layer-wise SROPs and useful information vary synchronously when model input and structures are different or training is sufficient. SROP is more rigorous because it contains less redundant information compared to ID. SROPs can be used to estimate channel-wise useful information, which has potential applications in various scenarios. SROPs are promising tools to explain the mechanism of DNNs with frequency-domain knowledge.

Acknowledgements

This work was supported by National Natural Science Foundation of China (81473579 and 81973744), Beijing Natural Science Foundation (7173267).

References

Convolutional Networks. <https://github.com/pytorch/examples/tree/master/mnist>. 5

Abdi, H. and Williams, L. Principal component analysis. *Wiley Interdisciplinary Reviews: Computational Statistics*, 2:433 – 459, 07 2010. 2

Adebayo, J., Gilmer, J., Muelly, M., Goodfellow, I., Hardt, M., and Kim, B. Sanity checks for saliency maps. In Bengio, S., Wallach, H., Larochelle, H., Grauman, K., Cesa-Bianchi, N., and Garnett,

R. (eds.), *Advances in Neural Information Processing Systems*, pp. 9505–9515. Curran Associates, Inc. 2, 4

Ansuini, A., Laio, A., Macke, J. H., and Zoccolan, D. Intrinsic dimension of data representations in deep neural networks. In *Advances in Neural Information Processing Systems*, pp. 6109–6119, 2019. 7

Arpit, D., Jastrzebski, S., Ballas, N., Krueger, D., Bengio, E., Kanwal, M. S., Maharaj, T., Fischer, A., Courville, A. C., Bengio, Y., and Lacoste-Julien, S. A closer look at memorization in deep networks. In *ICML*, 2017. 3

Badii, R. and Politi, A. Hausdorff dimension and uniformity factor of strange attractors. *Physical Review Letters - PHYS REV LETT*, 52:1661–1664, 05 1984. 2

Bengio, Y., Courville, A., and Vincent, P. Representation learning: A review and new perspectives. *IEEE Transactions on Pattern Analysis and Machine Intelligence*, 35(8):1798–1828, 2013. 2

Cheng, X., Rao, Z., Chen, Y., and Zhang, Q. Explaining knowledge distillation by quantifying the knowledge. In *2020 IEEE/CVF Conference on Computer Vision and Pattern Recognition (CVPR)*, pp. 12922–12932, 2020. 2

Cover, T. and Thomas, J. *Elements of information theory*. 2nd ed. 11 1990. ISBN 0-471-06259-6. 1

DeGroot, M. Uncertainty, information, and sequential experiments. *Annals of Mathematical Statistics*, 33, 06 1962. 2

Dieleman, S., De Fauw, J., and Kavukcuoglu, K. Exploiting cyclic symmetry in convolutional neural networks. In *Proceedings of the 33rd International Conference on International Conference on Machine Learning - Volume 48*, ICML'16, pp. 1889–1898. JMLR.org, 2016. 1

Facco, E., d'Errico, M., Rodriguez, A., and Laio, A. Estimating the intrinsic dimension of datasets by a minimal neighborhood information. *Scientific Reports*, 7, 12 2017. 2

Frankle, J. and Carbin, M. The lottery ticket hypothesis: Finding sparse, trainable neural networks. In *International Conference on Learning Representations*, 2019. 2

Goodfellow, I., Lee, H., Le, Q., Saxe, A., and Ng, A. Measuring invariances in deep networks. In Bengio, Y., Schuurmans, D., Lafferty, J., Williams, C., and Culotta, A. (eds.), *Advances in Neural Information Processing Systems*, pp. 646–654. Curran Associates, Inc. 1, 5

Ioffe, S. and Szegedy, C. Batch normalization: Accelerating deep network training by reducing internal covariate shift, 2015. 4, 6, 7

Jiang, Y., Neyshabur, B., Mobahi, H., Krishnan, D., and Bengio, S. Fantastic generalization measures and where to find them. In *8th International Conference on Learning Representations, ICLR 2020, Addis Ababa, Ethiopia, April 26-30, 2020*. Open-Review.net, 2020. 1

Koh, P. W. and Liang, P. Understanding black-box predictions via influence functions. volume 70 of *Proceedings of Machine Learning Research*, pp. 1885–1894, International Convention Centre, Sydney, Australia, 06–11 Aug 2017. PMLR. 1

Krizhevsky, A. Learning multiple layers of features from tiny images. *University of Toronto*, 05 2012. 3

Larochelle, H., Erhan, D., Courville, A., Bergstra, J., and Bengio, Y. An empirical evaluation of deep architectures on problems with many factors of variation. New York, NY, USA, 2007. Association for Computing Machinery. ISBN 9781595937933. 1

Lenc, K. and Vedaldi, A. Understanding image representations by measuring their equivariance and equivalence. In *2015 IEEE Conference on Computer Vision and Pattern Recognition (CVPR)*, pp. 991–999, 2015. 1

Lenzi, E., Mendes, R., and Silva, L. Statistical mechanics based on renyi entropy. *Physica A-statistical Mechanics and Its Applications - PHYSICA A*, 280:337–345, 06 2000. 2

Liang, R., Li, T., Li, L., Wang, J., and Zhang, Q. Knowledge consistency between neural networks and beyond, 2020. 2

Maus, S. The geomagnetic power spectrum. *Geophysical Journal International*, 174:135 – 142, 07 2008. 4

Negrea, J., Haghifam, M., Dziugaite, G. K., Khisti, A., and Roy, D. M. Information-theoretic generalization bounds for sgld via data-dependent estimates. In Wallach, H., Larochelle, H., Beygelzimer, A., d'Alché-Buc, F., Fox, E., and Garnett, R. (eds.), *Advances in Neural Information Processing Systems*, pp. 11015–11025. Curran Associates, Inc. 2

Paszke, A., Gross, S., Massa, F., Lerer, A., Bradbury, J., Chanan, G., et al. Pytorch: An imperative style, high-performance deep learning library. In Wallach, H., Larochelle, H., Beygelzimer, A., d'Alché-Buc, F., Fox, E., and Garnett, R. (eds.), *Advances in Neural Information Processing Systems 32*, pp. 8026–8037. Curran Associates, Inc. 5

Rahaman, N., Baratin, A., Arpit, D., Draxler, F., Lin, M., Hamplecht, F., Bengio, Y., and Courville, A. On the spectral bias of neural networks. In Chaudhuri, K. and Salakhutdinov, R. (eds.), *Proceedings of the 36th International Conference on Machine Learning*, volume 97 of *Proceedings of Machine Learning Research*, pp. 5301–5310, Long Beach, California, USA, 09–15 Jun 2019. PMLR. 3, 5

Russakovsky, O., Deng, J., Su, H., Krause, J., Satheesh, S., Ma, S., Huang, Z., Karpathy, A., Khosla, A., and Bernstein, M. Imagenet large scale visual recognition challenge. *International Journal of Computer Vision*, 115(3):211–252, 2015. 3

Scheirer, E. and Slaney, M. Construction and evaluation of a robust multifeature speech/music discriminator. volume 2, pp. 1331 – 1334 vol.2, 05 1997. 3

Shannon, C. and Weaver, W. *The Mathematical Theory of Communication (Introductory note)*. 01 1949. 1

Shwartz-Ziv, R. and Tishby, N. Opening the Black Box of Deep Neural Networks via Information. *arXiv e-prints*, March 2017. 7

Tan, M. and Le, Q. EfficientNet: Rethinking model scaling for convolutional neural networks. In Chaudhuri, K. and Salakhutdinov, R. (eds.), *Proceedings of the 36th International Conference on Machine Learning*, volume 97 of *Proceedings of Machine Learning Research*, pp. 6105–6114, Long Beach, California, USA, 09–15 Jun 2019. PMLR. 5

Tribello, G., Ceriotti, M., and Parrinello, M. Using sketch-map coordinates to analyze and bias molecular dynamics simulations. *Proceedings of the National Academy of Sciences of the United States of America*, 109:5196–5201, 01 2012. 2

Wang, H., Wu, X., Huang, Z., and Xing, E. P. High-frequency component helps explain the generalization of convolutional neural networks. In *2020 IEEE/CVF Conference on Computer Vision and Pattern Recognition, CVPR 2020, Seattle, WA, USA, June 13–19, 2020*, pp. 8681–8691. IEEE, 2020. 7

Xie, Z., Zhang, Z., Zhu, X., Huang, G., and Lin, S. Spatially adaptive inference with stochastic feature sampling and interpolation. *ArXiv*, abs/2003.08866, 2020. 2

Xu, K., Qin, M., Sun, F., Wang, Y., Chen, Y.-K., and Ren, F. Learning in the frequency domain. In *2020 IEEE/CVF Conference on Computer Vision and Pattern Recognition (CVPR)*, pp. 1737–1746, 2020a. 7

Xu, Y., Zhao, S., Song, J., Stewart, R., and Ermon, S. A theory of usable information under computational constraints. In *International Conference on Learning Representations*, 2020b. 1, 2

Xu, Z. J., Zhang, Y., and Xiao, Y. Training behavior of deep neural network in frequency domain. *CoRR*, abs/1807.01251, 2018. 3

Xu, Z. J., Zhang, Y., Luo, T., Xiao, Y., and Ma, Z. Frequency principle: Fourier analysis sheds light on deep neural networks. *CoRR*, abs/1901.06523, 2019. 3

Yak, S., Gonzalvo, J., and Mazzawi, H. Towards task and architecture-independent generalization gap predictors. *ArXiv*, abs/1906.01550, 2019. 1

Zhang, R. Making convolutional networks shift-invariant again. In Chaudhuri, K. and Salakhutdinov, R. (eds.), *Proceedings of the 36th International Conference on Machine Learning*, volume 97 of *Proceedings of Machine Learning Research*, pp. 7324–7334, Long Beach, California, USA, 09–15 Jun 2019. PMLR. 2, 3, 5, 7